



Universiteit
Leiden
The Netherlands

Transient interactions studied by NMR : iron sulfur proteins and their interaction partners

Xu, X.

Citation

Xu, X. (2009, January 21). *Transient interactions studied by NMR : iron sulfur proteins and their interaction partners*. Leiden. Retrieved from <https://hdl.handle.net/1887/13428>

Version: Corrected Publisher's Version

License: [Licence agreement concerning inclusion of doctoral thesis in the Institutional Repository of the University of Leiden](#)

Downloaded from: <https://hdl.handle.net/1887/13428>

Note: To cite this publication please use the final published version (if applicable).

**Intermolecular Dynamics Studied by Paramagnetic
Tagging**

Abstract

Yeast cytochrome *c* and bovine adrenodoxin form a dynamic electron transfer complex, which is a pure encounter complex. It was demonstrated that dynamic nature of the interaction can readily be probed by using a rigid lanthanide tag attached to cytochrome *c*. The tag, CLaNP-5, induces pseudocontact shifts and residual dipolar couplings and does not perturb the binding interface. Due to the dynamics in the complex, residual dipolar couplings in adrenodoxin are very small. Simulation shows that cytochrome *c* needs to sample a large part of the surface of adrenodoxin to explain the small degree of alignment observed for adrenodoxin. The method provides a simple and straightforward way to observe dynamics in protein complexes or domain-domain mobility without the need for external alignment media.

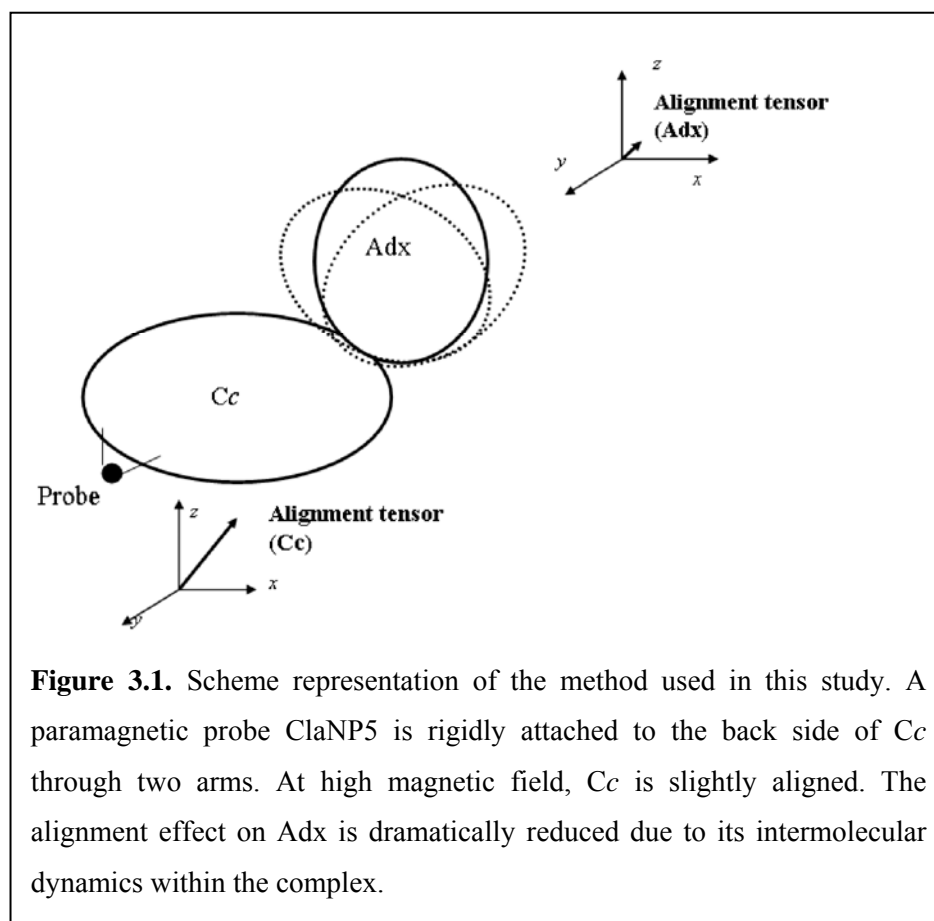
Introduction

Protein dynamics is important for protein function and recognition. Solution NMR is a powerful tool to study protein dynamics on the timescale ranging from pico-seconds to seconds. ^{15}N spin relaxation measurements combined with Liparo-Szabo analysis is now a standard NMR method to characterize the protein dynamics on ps-ns time scales ⁽²⁾. Recently, relaxation dispersion measurement has been developed as the powerful method to characterize the protein dynamics in μs -ms time scale ⁽³⁾. Residual dipolar couplings (RDCs) method initially emerged as a tool to provide useful long-range restraints for structure refinement. RDC is also sensitive to motions spanning the ps-ms time scale. Thus, the dynamics obtained from RDCs offer a view on dynamic processes that is complimentary to other NMR spectroscopic approaches ^(4,5,6).

RDCs can be measured when tumbling of biomolecules is slightly anisotropic. For some metalloproteins, weak molecular alignment can be achieved by paramagnetic susceptibility anisotropy in ultra high field ^(7,8). For other proteins, external alignment media have to be used ^(9,10,11). The interpretation of RDC data is difficult in the study of intermolecular dynamics, when an external alignment medium is used because the alignment tensors will be different for each conformation and the information obtained is only relative to the external magnetic field ⁽⁴⁾. In the study of bimolecular interaction involved with nucleic acids, the problem can be overcome by an elegant method in which an elongated RNA is used to obtain the alignment and a fixed reference frame was obtained for further RDC analysis ⁽¹²⁾. For protein-protein complexes or protein domain-domain interactions where two substructures are rigid, preferential alignment of one component and detection of RDCs on the other provides a more direct way for analysis of intermolecular dynamics ^(13,14).

Lanthanide paramagnetic probes offer an attractive way to achieve such partial alignment ⁽¹⁵⁾. Two-point attachment of a paramagnetic probe, Caged Lanthanide

NMR Probe 5 (CLaNP-5), through cysteine disulfide bridges proved to be a good way to introduce large and well-defined paramagnetic effects by minimizing the dynamics of probe ^(16,17).



In this study, CLaNP-5 is used to study the intermolecular dynamics of a dynamic complex of yeast cytochrome *c* (Cc) and bovine adrenodoxin (Adx). Adx is involved in steroid hormone biosynthesis by acting as an electron shuttle between NADPH-dependent adrenodoxin reductase and several cytochromes P450 ⁽¹⁸⁾. *In vitro* electron transfer from adrenodoxin reductase to Adx is often monitored by fast subsequent electron transfer from Adx to mitochondrial Cc.

The dynamical interaction between yeast *Cc* and bovine *Adx* was studied previously, demonstrating that the protein complex can be considered as a pure encounter complex ⁽¹⁹⁾. Large paramagnetic effects, including pseudocontact shifts (PCS) and RDCs are observed for the *Cc* when CLaNP-5 is rigidly attached. In the complex, very small RDC are detected on *Adx*, suggesting the averaging of multiple orientations of *Adx* relative to *Cc* due to large intermolecular dynamics (Figure 3.1). This method requires no external alignment media and also applicable for the study of dynamics in other protein complexes or between protein domains.

Materials and methods

Site-directed mutagenesis

Mutant *Cc*N56C/L58C was created by site-specific mutagenesis with overlap extension method ⁽²⁰⁾. The template DNA used for mutagenesis is pUC-cc containing the genes of yeast iso-1 *Cc* (C102T) and *Cc* heme lyase. The following four primers were used in three PCRs to amplify the mutated insert; M13 forward (5'-CCCAGTCACGACGTTGTAAAACG-3'), M13 reverse primer (5'-AGCGGATAACAATTTACACAGG-3'), N56C/L58C forward primer (5'-GCCAATATCAAGAAATGCGTGTGCTGGGACG-3') and N56C/L58C backward primer (5'-GTCCCAGCACACGCATTTCTTGATATTGGC-3'). The products of the third PCR was purified and subcloned into the *Xma*I/*Hind*III site of the plasmid pUC-18. The DNA sequence of pUC-ccN56C/L58C was verified by sequencing.

Protein production and ¹⁵N labeling

Double mutant *Cc*N56C/L58C was produced and purified using the same protocol as for wild type *Cc* ⁽¹⁹⁾. The final yield was 15 mg/L and 8 mg/L for the unlabeled and ¹⁵N labeled *Cc* mutant respectively. The concentration of *Cc*

mutant was determined using an extinction coefficient $27.5 \text{ mM}^{-1}\text{cm}^{-1}$ at 550 nm for the reduced *Cc* mutant. The production of both unlabeled and ^{15}N labeled Adx has been described⁽¹⁾.

Paramagnetic probe attachment

The synthesis of Ln-CLaNP-5 probe has been described⁽¹⁷⁾. To attach Ln-CLaNP-5 to *Cc*N56C/L58C, 600 μl 0.5 mM *Cc*N56C/L58C was first treated with DTT (final concentration 5 mM) at room temperature for 2 hrs to remove possible dimers by reduction of disulfide bonds. A PD-10 column (GE Healthcare) was used to remove the DTT and bring the protein in the 3 ml buffer containing 20 mM sodium phosphate and 150 mM NaCl, pH 7.0. Seven to ten equivalents CLaNP-5 were added and the solution was stirred for 2 hrs at 4 °C. The buffer was changed to 20 mM sodium phosphate, pH 7.0 before the solution was loaded on a HiTrap-SP column. The protein was eluted using a 350 to 700 mM NaCl gradient in 20 mM sodium phosphate, pH 7.0. Monomeric *Cc* attached to CLaNP-5 was concentrated and one equivalent of ascorbate was added to keep the *Cc* in reduced state. Either paramagnetic ytterbium or diamagnetic lutetium containing CLaNP-5 was attached to the *Cc* double mutant. The extent of probe attachment to ^{15}N *Cc*N56C/L58C was estimated to be above 90% from mass spectrometry and from the absence of diamagnetic crosspeaks in the HSQC spectra of the paramagnetic samples.

NMR spectroscopy

All NMR samples contained 20 mM potassium phosphate buffer, pH 7.4, 6 % D_2O and one eq. of ascorbic acid under an argon atmosphere to keep the *Cc* in the reduced state. Three sets of samples were prepared comprising free ^{15}N *Cc* with probe attached and the CLaNP-*Cc*/Adx (0.25 mM 1:1) complex in which either *Cc*N56C/L58C or Adx was ^{15}N labeled. Yb-CLaNP-5 was used in the paramagnetic samples and Lu-CLaNP-5 acted as a diamagnetic control. For

pseudocontact shift measurements, ^1H - ^{15}N HSQC spectra were recorded at 14.1 T on a Bruker DMX 600 MHz spectrometer equipped with a TCI-Z-GRAD cryoprobe operating at 293 K. For ^1H - ^{15}N RDC measurements, ^1H - ^{15}N IPAP-HSQC⁽²¹⁾ spectra were acquired at 21.1 T on a Bruker 900 spectrometer equipped with a TCI-Z-GRAD cryoprobe. RDC was obtained through the measurement of the splitting difference in the ^{15}N dimension between the samples containing paramagnetic Yb and diamagnetic Lu. NMR data were processed in Azara (www.bio.cam.ac.uk/azara), and analyzed in Ansig for Windows⁽²²⁾.

PCS and RDC analysis

The crystal structure of yeast iso-1 Cc (PDB entry: 1YCC⁽²³⁾) was used for PCS and RDC analysis. Hydrogens were added in XPLOR-NIH⁽²⁴⁾ according the standard geometry parameters. A set of pseudo-atoms representing the magnetic susceptibility tensor frame was added for the fit of PCS and RDC using PARAAstraints in XPLOR-NIH⁽²⁵⁾. The equation used for the tensor calculation is

$$PCS = \frac{1}{12\pi r^3} \left[\Delta\chi_{ax} (3\cos^2 \theta - 1) + \frac{3}{2} \Delta\chi_{rh} (\sin^2 \theta \cos 2\Omega) \right] \quad (1)$$

Where r , θ , and Ω are the polar coordinates of the nucleus with respect to the principle axes of the χ -tensor and $\Delta\chi_{ax}$ and $\Delta\chi_{rh}$ are the axial and rhombic components of the χ -tensor, respectively. The position of the lanthanide was determined by energy minimization PCS energy term and a term that restrained the metal to 6-10 Å from the C α of cysteines 56 and 58 of Cc⁽¹⁷⁾. The lowest-energy structure with the fewest PCS violations was used for further fitting of RDC using the FRUN algorithm in the PARAAstraints suite. The equation used for RDC alignment tensor determination is

$$D^{res} = -\frac{B_0^2}{15kT} \frac{\gamma_i \gamma_j h}{16\pi^3 r_{ij}^3} \left(\Delta\chi_{ax} (3 \cos^2 \theta - 1) + \frac{3}{2} \Delta\chi_{rh} \sin^2 \theta \cos 2\varphi \right) \quad (2)$$

Where B_0 is the applied magnetic field, γ_i and γ_j are the gyromagnetic ratios of nuclei i and j respectively, r is the i - j inter-nuclear distance (1.02 Å), θ and φ determine the inter-nuclear vector orientation with respect to the principle axes of the χ -tensor, $\Delta\chi_{ax}$ and $\Delta\chi_{rh}$ are the axial and rhombic components of the χ -tensor, respectively, and k and h are Boltzmann and Planck constants, respectively.

Simulation of the dynamics

The structure coordinates of Ln-Cc with optimized probe-metal center and magnetic susceptibility tensor frame and of Adx (PDB entry 1AYF⁽²⁶⁾) were used for simulations to explore the possible sampling space for averaging intermolecular RDCs. Similar to what described before ⁽¹⁹⁾, the relative diffusional movement of the proteins in the native complex was decomposed into two types of rotations. One is the rotation of Adx around its own center of mass (wobbling motion) and the other is the rotation of Adx around the Cc, resulting in the translational movement over its surface. The heme metal center of Cc was used as the rotating center for the second movement. Each rotation can be further decomposed into the rotations around the X, Y and Z axes. Six angle variables are thus used to describe the rotation ranges. The initial orientation of two proteins was generated in a way that N16 of Cc is in close contact with L80 of Adx. The initial distance of geometrical center of Adx to metal alignment center was set to 42 Å. This brings the proteins together in an orientation consistent with chemical shift perturbation data. The effect of averaging over the six rotating and wobbling axes was evaluated by generating 100 sterically allowed orientations randomly within a given angle range. The averaged intermolecular RDCs were calculated for amide protons of Adx in this

ensemble and compared with the observed RDCs for Adx in the complex.

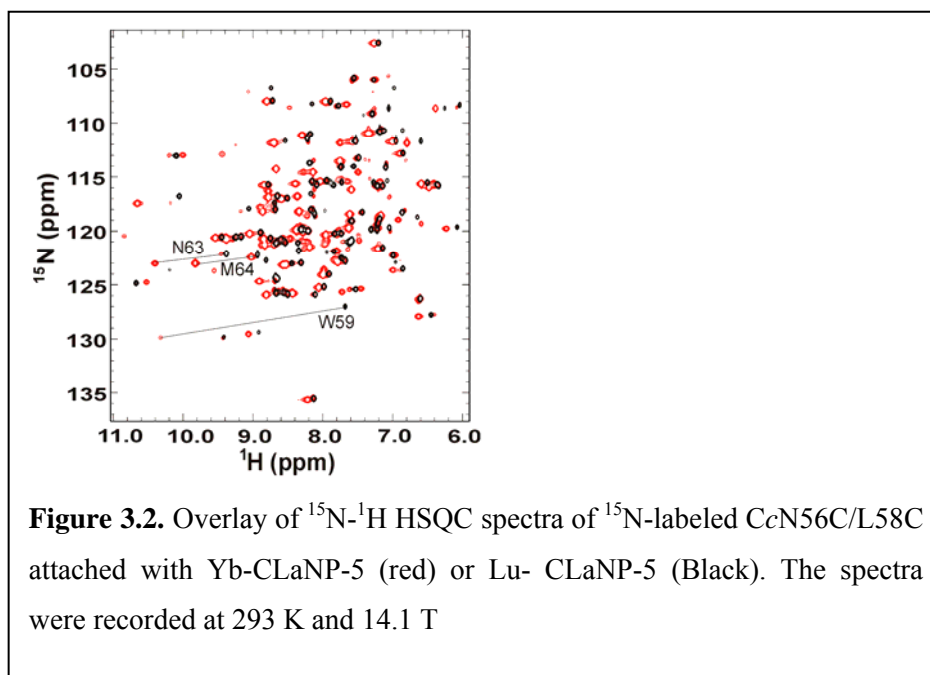
Results

Probe attachment on Cc

Two surface-exposed residues of Cc N56 and L58 were selected to be mutated to cysteines for the probe attachment. They are located on a short β -strand region (V57-W59) and at the back side of Cc with respect to heme edge region which is the interface involved in binding to various interaction partners^(27,28,29,30,31). The attachment of the probe to a site far from the interaction interface should cause little perturbation to the native interaction. The side chains of the two residues are 5-10 Å apart which is an optimal distance for the two arms of the CLaNP probe. Via two disulfide bridges formed between the cysteine residues and two arms of Ln-probe, the probe was rigidly attached to protein surface. The molecular weight of purified product of Lu-CLaNP ¹⁵N Cc (13547.9 ± 1 Da) agrees with the theoretical molecular weight (13548.2 Da). Two disulfide bridges formation was confirmed by mass spectroscopy. The yield of the entire labeling procedure from probe attachment to purification is about 50%.

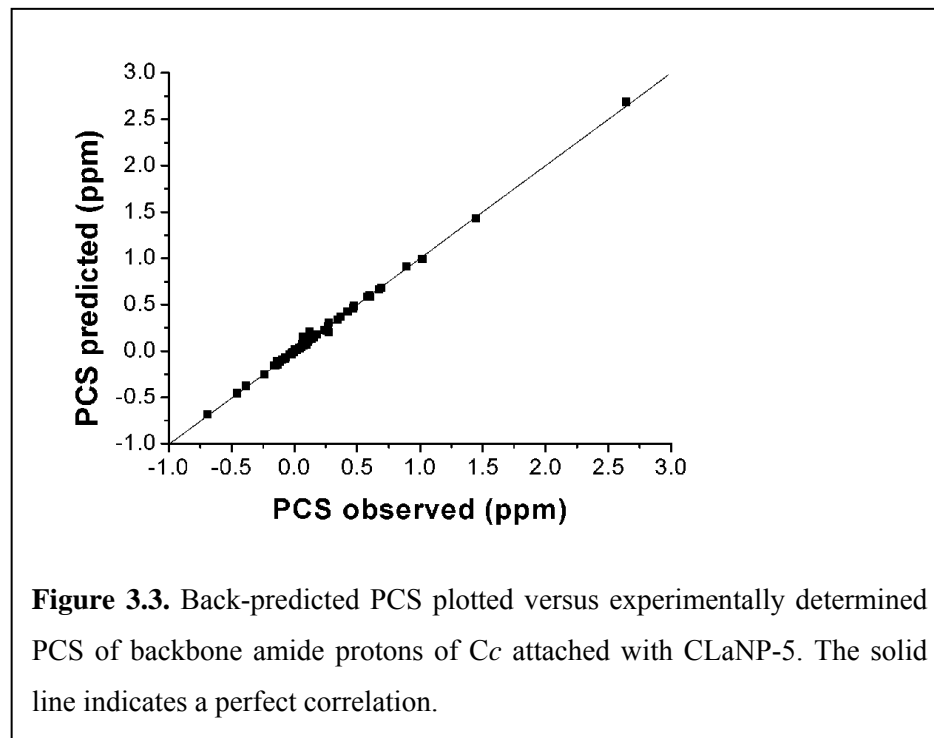
Magnetic susceptibility tensor determination

The ¹⁵N-HSQC of Lu-Cc is similar to that of wt Cc except for a few residues in close proximity to sites of mutation, indicating that the probe attachment does not cause large perturbations of the structure. PCSs were caused by the dipolar interaction between the unpaired electron of the lanthanide ion and the nuclei of



Cc and were measured by comparison of HSQC spectra for samples with diamagnetic Lu and paramagnetic Yb-CLaNP-5. A single set of PCSs was observed for Yb-Cc as compared to Lu-Cc, confirming the attachment of probe to protein by two disulfide bridges. For each backbone amide ^1H and ^{15}N pair far from the metal site, similar PCSs are expected (in ppm) for the ^1H and ^{15}N nuclei. This leads to the unambiguous assignment of some backbone amides at initial stage, allowing magnetic susceptibility tensor determination and subsequent assignment of more residues by an iterative procedure. The largest PCS (> 2 ppm) was detected for the amide proton of W59 of Cc (Figure 3.2). In total, 73 amide protons of reduced Cc with probe attached were assigned and used for magnetic susceptibility tensor ($\Delta\chi$) determination by fitting with the crystal structure of yeast Cc (1YCC). The size of axial and rhombic components ($\Delta\chi_{\text{ax}}$ and $\Delta\chi_{\text{rh}}$ in 10^{-32} m^3) were 8.3 ± 0.2 and 3.1 ± 0.2 respectively. Figure 3.3 shows a correlation plot of experimentally observed and theoretically predicted

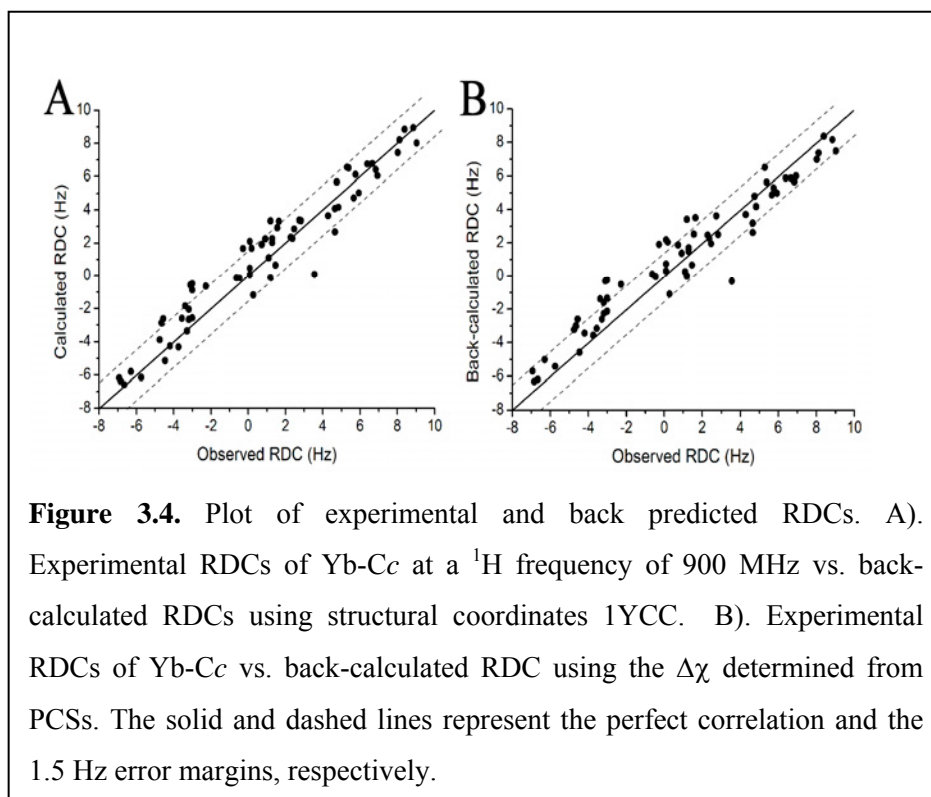
PCS. The good fit (Q factor: 0.047) support the finding that CLaNP is rigid relative to the frame of the protein.



Magnetically induced RDC

Magnetic field induced RDC scales with the squared value of magnetic field strength. At 900 MHz magnetic field, RDC as large as 9 Hz was detected for *Cc* attached with Yb-probe. The alignment tensor was determined using 64 RDCs of N-H pairs of *Cc*. Due to the large uncertainty of RDC measurement at 900 MHz, 1.5 Hz was used as the error for fitting. Figure 3.4A shows the correlation for experimental and back calculated RDC by fitting to the crystal structure of *Cc* (Q factor 0.263). The correlation is acceptable given the error margins and the fact that the crystal structure was not refined using the RDC data. The fitted alignment tensor is 6.71 and 2.0 (in 10^{-32} m^3) for axial and rhombic components, respectively. The axial component value fitted from RDC is about 19% smaller

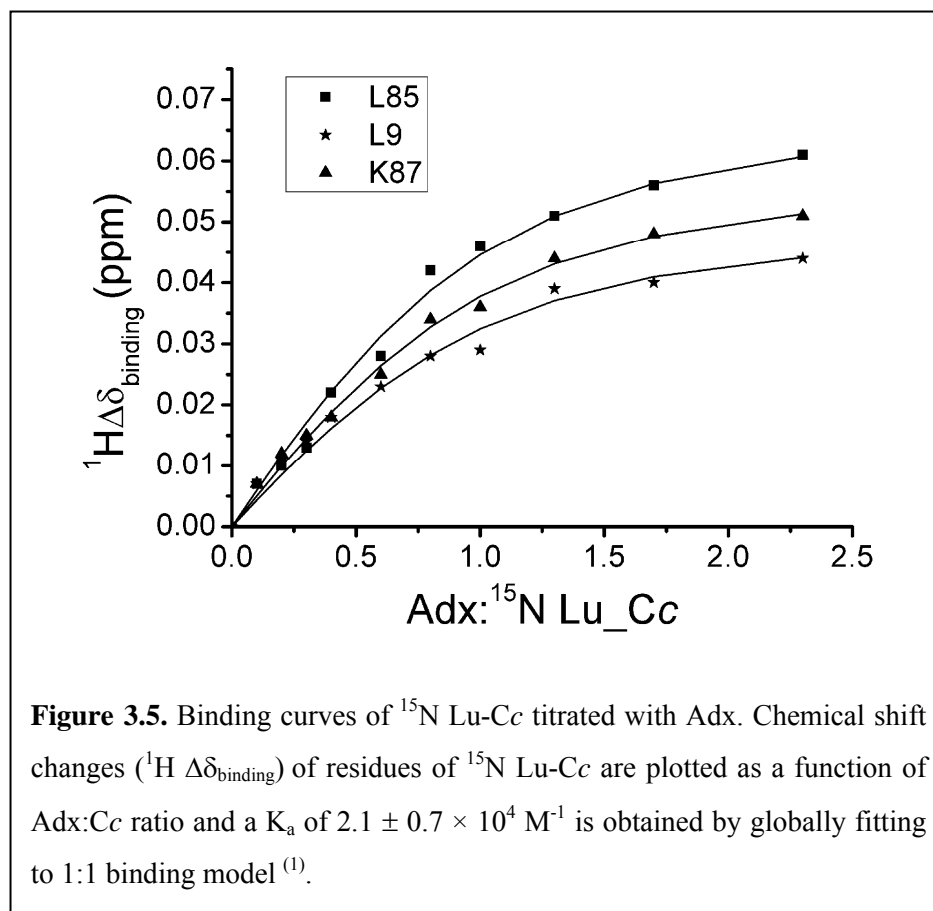
from the one of PCS. The correlation between observed RDCs and RDCs back-calculated using the PCS tensor values is shown in Figure 3.4B. The Q factor is 0.287, only slightly larger than the fitted tensor. Thus, it could be that the difference between the $\Delta\chi$ values derived from RDCs and PCSs is not significant. Alternatively, this could be attributable to internal dynamics because RDCs are more sensitive to the internal dynamics than PCS. The dynamics may represent mobility of the probe, but could also be caused by mobility of amide groups⁽³²⁾.



The interaction of Ln-Cc with Adx

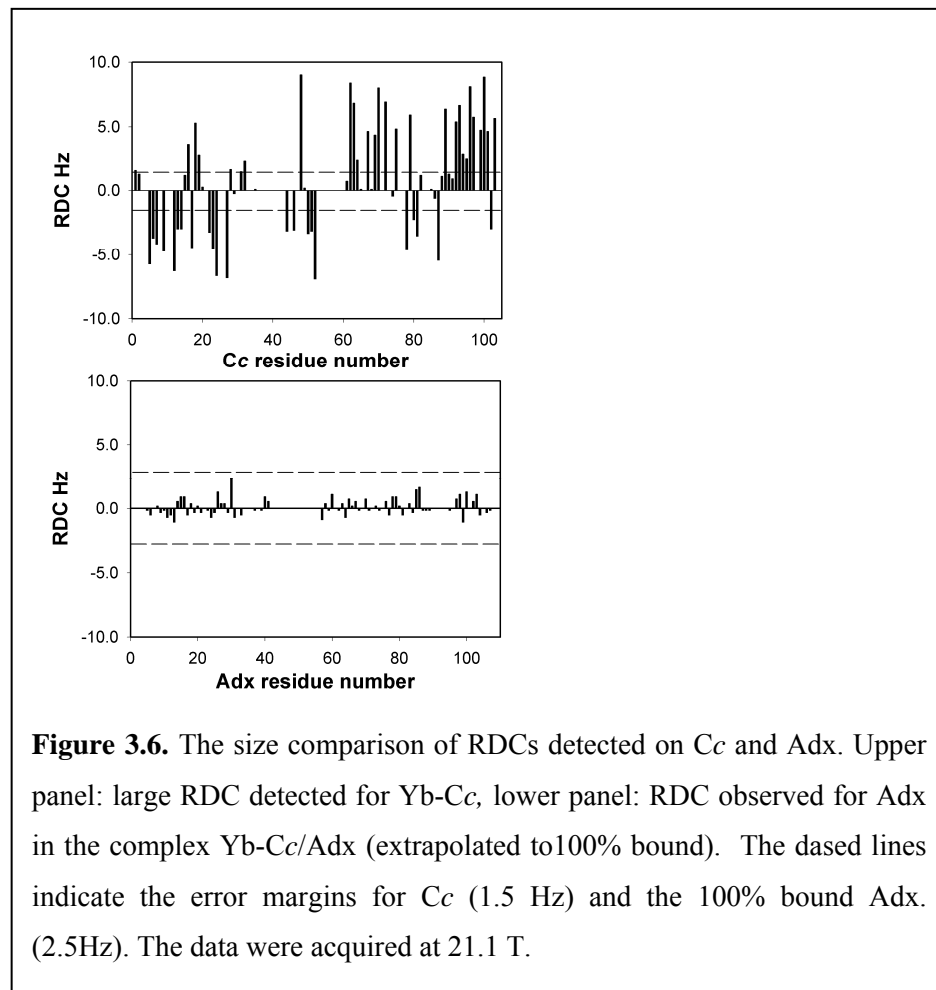
The interface of Ln-Cc determined from chemical shift perturbations is similar to that in the native complex. The titration experiment of unlabeled Adx to ^{15}N

Lu-Cc yielded a K_a value $2.1 (\pm 0.7) \times 10^4 \text{ M}^{-1}$ of interaction of Ln-Cc with Adx (Figure 3.5), which is slightly changed comparing to that ($4.0 \pm 1.0 \times 10^4 \text{ M}^{-1}$) of the wild type Cc/Adx interaction ⁽¹⁾, possibly due to the small temperature difference of the measurements. Using the ^{15}N labeled Cc attached with CLaNP-5, both PCSs and RDCs were measured for Cc in the complex Cc/Adx. In the 1:1 complex of CLaNP5-Cc/Adx, the observed PCSs and RDCs for Cc are the weighted average of free and complex states. The comparison of PCSs and RDCs values for free Yb-Cc and Yb-Cc in the complex clearly suggests that magnetic susceptibility tensor does not change with the complex formation.



Small paramagnetic effects on Adx in the Cc/Adx complex

When the Ln-Cc interacts with ^{15}N Adx, the paramagnetic effects observed for



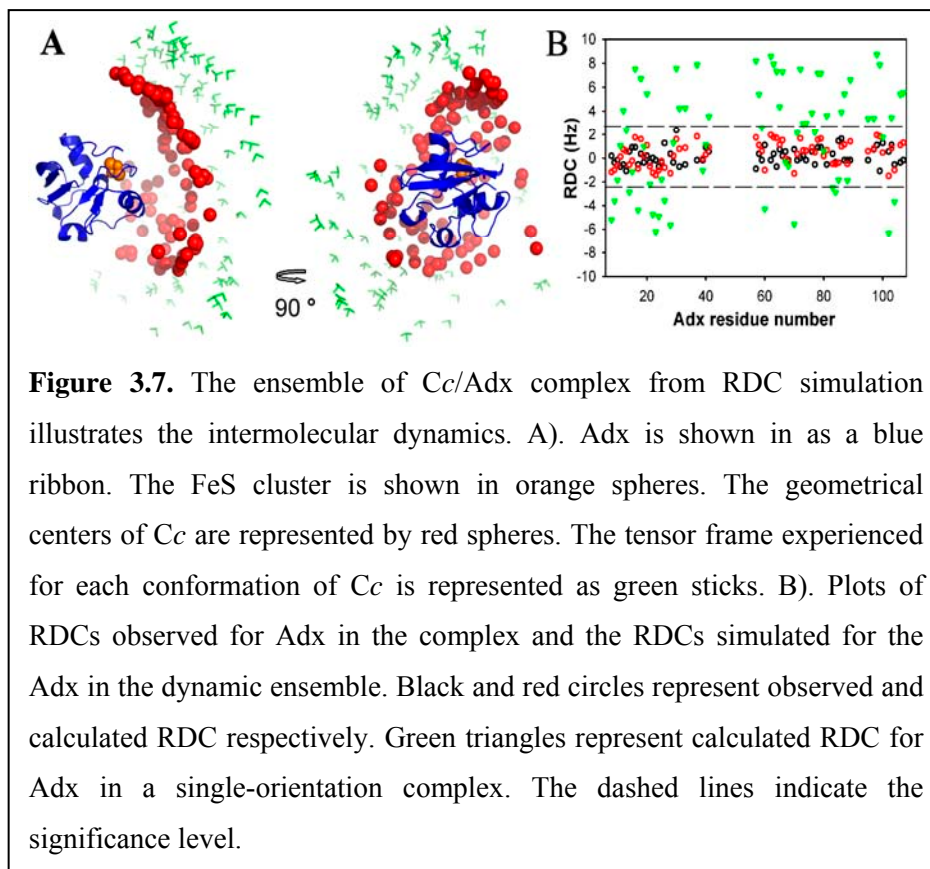
Adx are the weighted average of the effect for Adx in free and complex state. At the ratio of 1:1 Adx/Ln-*Cc* (0.25 mM), about 61% Adx is in the complex state. According to the equation 1, only small PCSs are expected for a few residues of Adx even in the single-orientation complex because the Ln metal center is relatively far ($> 35 \text{ \AA}$) from most of the residues of Adx. However, RDCs are only angular-dependent. If the alignment of Adx in the complex is the same as for Yb-*Cc*, RDCs of 4-5 Hz are expected, and when extrapolated to 100%,

values up to 9 Hz are predicted. The largest extrapolated RDC observed for Adx in 100% bound state is about 2 Hz (Figure 3.6), which is much smaller than the RDCs determined for Cc and below the significance level. The striking difference of RDC values detected for Adx and Cc in the complex is in accord with the intermolecular dynamics between Cc and Adx in the complex.

Intermolecular dynamics from RDC simulation

A simulation was performed to explore the magnitude of the intermolecular motions in the complex. The movement of two proteins in the dynamics in the complex was decomposed into six different rotations. Within a set sampling space, all sterically-allowed conformations were randomly sampled. In this way, ensembles of the protein complexes were generated and compared with the observed NMR parameters including chemical shift perturbations and RDCs. In any single-orientation conformation of Ln-Cc/Adx, the predicted largest RDCs for amide protons of Adx are as large as $\pm 8-9$ Hz, similar to those detected for Cc. The insignificant RDCs observed for Adx in the complex are the direct result of intermolecular dynamics, which can average the N-H bond orientations relative to the reference frame for the dynamic ensemble. The simulation suggests that the rotation of Adx around Cc (translational movement of Adx on Cc heme edge) hardly reduced the averaged RDC values on Adx. This is in contrast to the large averaging effect of the same movement on PCS originating from heme center in the previous study⁽¹⁹⁾. The rotation of Adx around its own geometrical center can lead to a large change of N-H inter-nuclear vector orientation (θ and Ω) with respect to the principle axes of the magnetic susceptibility tensor, thus averaging the RDC to an insignificant scale. In an ensemble with RDC averaged out, Cc needs to sample a large surface area of Adx (Figure 3.7A). The sampling space in this ensemble agrees well with the chemical shift perturbation data and is also consistent with our previous study

using the internal heme site of Cc and spin labeling as paramagnetic probes⁽¹⁹⁾.



Discussion

Paramagnetic metal ions provide NMR effects such as paramagnetic relaxation enhancement (PRE), PCS and RDC due to self-orientation in high magnetic field. These effects can be converted into distance or angular restraints which are useful not only for structure determination, but also for the study of dynamics. PRE is isotropic and reversely dependent on the metal-nucleus distance ($1/r^6$ dependence) and shows fast decay. Therefore, PRE is powerful to detect minor population in a heterogeneous system^(33,34,35). PCS depends on the metal-nucleus

orientation and distance, decaying with $1/r^3$. The magnitude of metal-induced RDCs is not dependent on metal-nucleus distance, thus each of these observables provides a different view on the dynamics in the system. PCSs and RDCs exhibit averaging for all motions occurring on a time scale faster than 10^{-2} s.

For a two-component system (two domains or proteins), where an external medium is used to obtain weak alignment for RDC measurement, the intermolecular dynamics may be implied from the different ordering tensors experienced by the two components^(36,37). Failure to observe such a difference however, does not exclude the dynamics. The difficulty associated with studies of intermolecular dynamics is that the motions may change the alignment frame of each instantaneous conformation. One approach to overcoming this problem is the metal-induced alignment, which can provide a fixed reference alignment frame for one component of the interaction system. This method already proved to be useful to obtain information on dynamics of domain-domain interactions of metallo-proteins^(13,38). To extend this method to other diamagnetic proteins without metal sites, a paramagnetic tag is needed to be attached rigidly to the protein surface.

CLaNP-5 has been shown to exhibit minimized internal dynamics through attachment via two disulfides bridges^(16,17). In this study, the Yb-CLaNP-5 was rigidly attached to the back side of reduced Cc (diamagnetic form) to obtain large PCSs and RDCs, with much smaller paramagnetic effects observed for Adx in the dynamic complex. Among all Ln metals, Yb is classified as moderately paramagnetic but with a small broadening effect. Other highly paramagnetic Ln metals (Dy, Tb, Tm) which induce larger PCSs and RDCs⁽¹⁷⁾, can provide more extensive datasets for accurately modeling the 3-D sampling space of the dynamic complex. Although in this study two metalloproteins were involved, this method should be generally applicable to other protein complexes

or multiple-domain proteins without metal-binding sites, because the heme and FeS cluster were not used in this study in any way.

Acknowledgement

Financial support was provided by the Fonds der chem. Industrie the Volkswagenstiftung grant and the Netherlands Organization for Scientific Research. RDC measurement was carried out on a 900 MHz spectrometer in the NMR facility of the Bijvoet Center in Utrecht and Dr H. Wienk is acknowledged for the technical help on NMR measurements. Hans van der Elst is acknowledged for assistance with MS measurements.

Reference List

1. Worrall J.A.R., Reinle W., Bernhardt R., and Ubbink M. (2003) Transient protein interactions studied by NMR spectroscopy: The case of cytochrome *c* and adrenodoxin. *Biochemistry* **42**: 7068-7076.
2. Palmer A.G. (2004) NMR characterization of the dynamics of biomacromolecules. *Chem.Rev.* **104**: 3623-3640.
3. Korzhnev D.M. and Kay L.E. (2008) Probing invisible, low-populated states of protein molecules by relaxation dispersion NMR spectroscopy: An application to protein folding. *Acc.Chem.Res.* **41**: 442-451.
4. Tolman J.R. and Ruan K. (2006) NMR residual dipolar couplings as probes of biomolecular dynamics. *Chem.Rev.* **106**: 1720-1736.
5. Lakomek N.A., Walter K.F.A., Fares C., Lange O.F., de Groot B.L., Grubmuller H., Bruschweiler R., Munk A., Becker S., Meiler J., and Griesinger C. (2008) Self-consistent residual dipolar coupling based model-free analysis for the robust determination of nanosecond to microsecond protein dynamics. *J.Biomol.NMR* **41**: 139-155.
6. Lange O.F., Lakomek N.A., Fares C., Schroder G.F., Walter K.F.A., Becker S., Meiler J., Grubmuller H., Griesinger C., and de Groot B.L. (2008) Recognition dynamics up to microseconds revealed from an RDC-derived ubiquitin ensemble in solution. *Science* **320**: 1471-1475.
7. Tolman J.R., Flanagan J.M., Kennedy M.A., and Prestegard J.H. (1995) Nuclear magnetic dipole interactions in field-oriented proteins - information for structure determination in solution. *Proc.Natl.Acad.Sci.U.S.A.* **92**: 9279-9283.
8. Banci L., Bertini I., Huber J.G., Luchinat C., and Rosato A. (1998) Partial orientation of oxidized and reduced cytochrome *b₅* at high magnetic fields: Magnetic susceptibility

- anisotropy contributions and consequences for protein solution structure determination. *J.Am.Chem.Soc.* **120**: 12903-12909.
9. Tjandra N. and Bax A. (1997) Direct measurement of distances and angles in biomolecules by NMR in a dilute liquid crystalline medium. *Science* **278**: 1111-1114.
 10. Tjandra N., Omichinski J.G., Gronenborn A.M., Clore G.M., and Bax A. (1997) Use of dipolar ^1H - ^{15}N and ^1H - ^{13}C couplings in the structure determination of magnetically oriented macromolecules in solution. *Nat.Struct.Biol.* **4**: 732-738.
 11. Bax A. and Grishaev A. (2005) Weak alignment NMR: a hawk-eyed view of biomolecular structure. *Curr.Opin.Struct.Biol.* **15**: 563-570.
 12. Zhang Q., Stelzer A.C., Fisher C.K., and Al Hashimi H.M. (2007) Visualizing spatially correlated dynamics that directs RNA conformational transitions. *Nature* **450**: 1263-1267.
 13. Bertini I., Del Bianco C., Gelis I., Katsaros N., Luchinat C., Parigi G., Peana M., Provenzani A., and Zoroddu M.A. (2004) Experimentally exploring the conformational space sampled by domain reorientation in calmodulin. *Proc.Natl.Acad.Sci.U.S.A.* **101**: 6841-6846.
 14. Rodriguez-Castaneda F., Haberz P., Leonov A., and Griesinger C. (2006) Paramagnetic tagging of diamagnetic proteins for solution NMR. *Magn.Reson.Chem.* **44**: S10-S16.
 15. Otting G. (2008) Prospects for lanthanides in structural biology by NMR. *J.Biomol.NMR* **42**: 1-9.
 16. Keizers P.H.J., Desreux J.F., Overhand M., and Ubbink M. (2007) Increased paramagnetic effect of a lanthanide protein probe by two-point attachment. *J.Am.Chem.Soc.* **129**: 9292-+.
 17. Keizers P.H., Saragliadis A., Hiruma Y., Overhand M., and Ubbink M. (2008) Design, Synthesis, and Evaluation of a Lanthanide Chelating Protein Probe: CLaNP-5 Yields Predictable Paramagnetic Effects Independent of Environment. *J.Am.Chem.Soc.* **130**: 14802-14812.
 18. Grinberg A.V., Hannemann F., Schiffler B., Müller J., Heinemann U., and Bernhardt R. (2000) Adrenodoxin: Structure, stability, and electron transfer properties. *Proteins-Structure Function and Genetics* **40**: 590-612.
 19. Xu X.F., Reinle W.G., Hannemann F., Konarev P.V., Svergun D.I., Bernhardt R., and Ubbink M. (2008) Dynamics in a pure encounter complex of two proteins studied by solution scattering and paramagnetic NMR spectroscopy. *J.Am.Chem.Soc.* **130**: 6395-6403.
 20. Ho S.N., Hunt H.D., Horton R.M., Pullen J.K., and Pease L.R. (1989) Site-Directed Mutagenesis by Overlap Extension Using the Polymerase Chain-Reaction. *Gene* **77**: 51-59.
 21. Ottiger M., Delaglio F., and Bax A. (1998) Measurement of J and dipolar couplings from simplified two-dimensional NMR spectra. *J.Magn.Reson.* **131**: 373-378.
 22. Helgstrand M., Kraulis P., Allard P., and Härd T. (2000) Ansig for Windows: An interactive computer program for semiautomatic assignment of protein NMR spectra. *J.Biomol.NMR* **18**: 329-336.
 23. Louie G.V. and Brayer G.D. (1990) High-resolution refinement of yeast iso-1-cytochrome c and comparisons with other eukaryotic cytochromes c. *J.Mol.Biol.* **214**: 527-555.
 24. Schwieters C.D., Kuszewski J.J., Tjandra N., and Clore G.M. (2003) The Xplor-NIH NMR molecular structure determination package. *J.Magn.Reson.* **160**: 65-73.
 25. Banci L., Bertini I., Cavallaro G., Giachetti A., Luchinat C., and Parigi G. (2004) Paramagnetism-based restraints for Xplor-NIH. *J.Biomol.NMR* **28**: 249-261.
 26. Müller A., Müller J., Müller Y., Uhlman, H., Bernhard, R., and Heineman (1998) New aspects of electron transfer revealed by the crystal structure of a truncated bovine adrenodoxin, Adx(4-108). *Structure* **6**: 269-280.
 27. Ubbink M. and Bendall D.S. (1997) Complex of plastocyanin and cytochrome c characterized by NMR chemical shift analysis. *Biochemistry* **36**: 6326-6335.
 28. Worrall J.A.R., Kolczak U., Canters G.W., and Ubbink M. (2001) Interaction of yeast iso-1-cytochrome c with cytochrome c peroxidase investigated by [^{15}N , ^1H] heteronuclear NMR spectroscopy. *Biochemistry* **40**: 7069-7076.

29. Crowley P.B., Rabe K.S., Worrall J.A.R., Canters G.W., and Ubbink M. (2002) The ternary complex of cytochrome *f* and cytochrome *c*: Identification of a second binding site and competition for plastocyanin binding. *ChemBiochem* **3**: 526-533.
30. Banci L., Bertini I., Felli I.C., Krippahl L., Kubicek K., Moura J.J.G., and Rosato A. (2003) A further investigation of the cytochrome *b₅* cytochrome *c* complex. *J.Biol.Inorg.Chem.* **8**: 777-786.
31. Volkov A.N., Ferrari D., Worrall J.A.R., Bonvin A.M.J.J., and Ubbink M. (2005) The orientations of cytochrome *c* in the highly dynamic complex with cytochrome *b₅* visualized by NMR and docking using HADDOCK. *Prot.Sci.* **14**: 799-811.
32. Bouvignies G., Bernado P., and Blackledge M. (2005) Protein backbone dynamics from N-H-N dipolar couplings in partially aligned systems: a comparison of motional models in the presence of structural noise. *J.Magn.Reson.* **173**: 328-338.
33. Tang C., Iwahara J., and Clore G.M. (2006) Visualization of transient encounter complexes in protein-protein association. *Nature* **444**: 383-386.
34. Tang C., Schwieters C.D., and Clore G.M. (2007) Open-to-closed transition in apo maltose-binding protein observed by paramagnetic NMR. *Nature* **449**: 1078-1082.
35. Volkov A.N., Worrall J.A.R., Holtzmann E., and Ubbink M. (2006) Solution structure and dynamics of the complex between cytochrome *c* and cytochrome *c* peroxidase determined by paramagnetic NMR. *Proc.Natl.Acad.Sci.U.S.A.* **103**: 18945-18950.
36. Braddock D.T., Louis J.M., Baber J.L., Levens D., and Clore G.M. (2002) Structure and dynamics of KH domains from FBP bound to single-stranded DNA. *Nature* **415**: 1051-1056.
37. Ulmer T.S., Werner J.M., and Campbell I.D. (2002) SH3-SH2 domain orientation in Src kinases: NMR studies of Fyn. *Structure* **10**: 901-911.
38. Bertini I., Gupta Y.K., Luchinat C., Parigi G., Peana M., Sgheri L., and Yuan J. (2007) Paramagnetism-based NMR restraints provide maximum allowed probabilities for the different conformations of partially independent protein domains. *J.Am.Chem.Soc.* **129**: 12786-12794.